

Exact Mixed-Integer Programming Approach for Chance-Constrained Multi-Area Reserve Sizing

Jehum Cho, Anthony Papavasiliou, *Senior Member, IEEE*,

Abstract—An exact algorithm is developed for the chance-constrained multi-area reserve sizing problem in the presence of transmission network constraints. The problem can be cast as a two-stage stochastic mixed integer linear program using sample approximation. Due to the complicated structure of the problem, existing methods attempt to find a feasible solution based on heuristics. Existing mixed-integer algorithms that can be applied directly to a two-stage stochastic program can only address small-scale problems that are not practical. We have found the minimal description of the projection of our problem onto the space of the first-stage variables. This enables us to directly apply more general Integer Programming techniques for mixing sets, that arise in chance-constrained problems. Our method can tackle real-world problems. We specifically consider a case study of the 10-zone Nordic network with 100,000 scenarios where the optimal solution can be found in approximately 5 minutes.

Index Terms—Multi-area reserve sizing, chance constraints, probabilistic constraints, mixed-integer programming

I. INTRODUCTION

In Europe, transmission system operators (TSOs) are increasingly coordinating their system operations in response to the pan-European coupling of electricity markets [1]. One of the objectives of this coupling is to organize a system that encompasses multiple areas for dispatching balancing energy from frequency restoration reserves in real time or close to real time (the MARI and PICASSO platforms)¹. An important problem of interest which is emerging as a result of cross-zonal coordination in balancing is to allocate the right quantities of reserves in the right locations of the network, while accounting for possible congestion in the transmission network. This problem is referred to as reserve sizing or reserve dimensioning, with the associated challenge of reserve deliverability [2], [3], depending on the context.

Article 157 of the System Operation Guideline (SOG) of the European Union [4] explicitly specifies probabilistic requirements for reserve sizing. The Nordic System Operation Agreement (SOA) [5] is an example of an effort for the coordinated operation of frequency reserves among the Nordic countries in response to the SOGL.

There are a number of papers in the literature that are related to this problem [6]–[10]. However, none of them address chance constraints and transmission constraints simultaneously without approximations of probabilistic distributions except for [11]. Although [11] accounts for both of these characteristics of the multi-area reserve sizing problem and

defines a chance-constrained formulation for the problem, the authors suggest a heuristic method that cannot guarantee to be optimal. Subsequent work attempts to solve this two-stage mixed-integer programming to optimality by applying integer programming techniques [12]. However, this method is not scalable to the size of realistic problems.

Starting from [14], there exists a strand of literature about using integer programming techniques for solving chance-constrained optimization problems [15]–[24]. However, not all of these methods can be directly applied to our problem. Most of them are designed for one-stage joint² chance-constrained problems. Our problem is formulated as a two-stage chance-constrained problem to which only some of them [17], [18], [20] are applicable. Even with them, using general methods straightforwardly does not perform well with large-scaled problems. For example, [12] is based on the method in [17] and this method is not scalable. In this paper, we propose an exact mixed-integer programming approach that is practically applicable. Instead of directly applying general methods for two-stage chance-constrained problems, we provide a novel minimal projection formulation. This projection formulation enables us to use more powerful integer programming techniques for joint chance-constrained problems such as [14]–[16], [22]–[24].

In general, finding a projection from a space with a higher dimension is difficult. Applying general purpose projection methods [25]–[27] requires a prohibitive amount of computation, especially for large-scale instances. In this paper, we provide a closed-form minimal projection formulation. This allows us to develop a method that is scalable to realistic problems, as we demonstrate in a case study at the end of the paper.

In section II, we present a formal definition of our problem and compare different formulations that are equivalent. First, we introduce a formulation from [11] that is used for their heuristic method. Later, we introduce our minimal projection formulation. In section III, we introduce integer programming techniques related to mixing inequalities. First, we start from general concepts and a Branch-and-Cut algorithm that can be directly applicable to a two-stage chance-constrained problem. Then, we present a related but slightly different approach that we use for our method. In section IV, we formally present our strengthened minimal projection formulation which is a combination of the minimal projection formulation in section II and the integer programming techniques introduced in section

¹MARI stands for “Manually Activated Reserves Initiative”, PICASSO stands for “Platform for the International Coordination of Automated Frequency Restoration and Stable System Operation”.

²The term *joint* comes from the fact that a probabilistic requirement is imposed on multiple constraints simultaneously.

III. Detailed explanations for implementing our algorithm are provided in this section. In section V, a realistic case study of the Nordic system is presented. We compare our method with the heuristic from [11] for varying levels of system reliability. In-depth simulation results over different sample sizes are also presented. Section VI summarizes the paper and propose areas of future research.

II. PROBLEM FORMULATIONS

For a network $\mathcal{G}(Z, E)$, let r_z^+ [resp. r_z^-] denote the size of upward [resp. downward] balancing capacity of reserve for each zone z . Our goal is to minimize the sum of r_z^+ and r_z^- for all the zones in $\mathcal{G}(Z, E)$. Note that the objective function can be extended straightforwardly to the case where total procurement costs are considered through balancing capacity offers. In that case, the coefficients of $r_z^{+/-}$ would be different values from one, but the method in this paper can manage this type of adjustment. F^+ [resp. F^-] denotes the feasible region for r^+ [resp. r^-] representing the region where the capacity of reserve can cover imbalances δ_z for each zone z in the network $\mathcal{G}(Z, E)$. Formally, $F^{+/-}$ are defined as (1) and (2).

$$F^+ = \{r^+ \in \mathbb{R}_+^{|Z|} : \exists(p, f) \text{ s.t.} \\ p_z + \delta_z = \sum_{e=(z, \cdot) \in E} f_e - \sum_{e=(\cdot, z) \in E} f_e, \quad \forall z \in Z \\ p_z \leq r_z^+, \quad \forall z \in Z \\ -T_e^- \leq f_e \leq T_e^+, \quad \forall e \in E\} \quad (1)$$

$$F^- = \{r^- \in \mathbb{R}_+^{|Z|} : \exists(p, f) \text{ s.t.} \\ p_z + \delta_z = \sum_{e=(z, \cdot) \in E} f_e - \sum_{e=(\cdot, z) \in E} f_e, \quad \forall z \in Z \\ -r_z^- \leq p_z, \quad \forall z \in Z \\ -T_e^- \leq f_e \leq T_e^+, \quad \forall e \in E\} \quad (2)$$

Here, p_z and f_e are the amount of balancing energy activated at zone z and the flow from z_1 to z_2 , where $e = (z_1, z_2)$, given that link e has capacity limits T_e^+ and T_e^- in the reference and opposite direction respectively. Notice that the values of δ_z , $T_e^{+/-}$ can vary under different scenarios, as we discuss in the sequel.

Notice that, in this paper, we assume that power flow constraints are approximated using a transportation network model. This assumption is aligned with the fact that within MARI, the platform for the activation of manual frequency restoration reserve, the network will be approximated using an ATC (Available Transfer Capacity) transportation-based model [28], [29] at the launch of the platform.

Given reliability targets for upward/downward reserves $(1 - \epsilon^{+/-})$, our problem can be written with probabilistic constraints (3b) as follows.

$$\min \sum_{z \in Z} (r_z^+ + r_z^-) \quad (3a)$$

$$\text{s.t. } \Pr\{r^{+/-} \in F^{+/-}\} \geq 1 - \epsilon^{+/-} \quad (3b)$$

$$r^{+/-} \geq 0 \quad (3c)$$

This is a two-stage chance-constrained formulation where the first-stage variables are r^+ , r^- and the second-stage variables are p_z and f_e . There are two different directions that

we consider for reformulating the constraints (3b). First, we directly use the second-stage variables p_z and f_e in order to represent $r^{+/-} \in F^{+/-}$. Second, we use a projection method to represent the feasible regions of the first-stage variables r^+ , r^- explicitly in the space of the first-stage variables.

A. Big-M Based Formulation with Second-Stage Variables

A common way to formulate this problem is to use a “big-M method” and the sample approximation approach introduced in [13] in order to represent the probabilistic constraints (3b). Given a positive integer n , let us denote $[n]$ as the set $\{1, \dots, n\}$. For $i \in [N]$, δ_{zi} denotes the imbalance of scenario i at zone z and $T_{ei}^{+/-}$ the transmission network capacities of line e for scenario i . By introducing new variables $u^{+/-}$ and $l^{+/-}$, our problem can be reformulated as follows.

$$\begin{aligned} \min \sum_{z \in Z} (r_z^+ + r_z^-) \\ \text{s.t. } p_{zi} + l_{zi}^+ - l_{zi}^- + \delta_{zi} &= \sum_{e=(z, \cdot) \in E} f_{ei} \\ &- \sum_{e=(\cdot, z) \in E} f_{ei}, \quad \forall z \in Z, i \in [N] \\ -r_z^- &\leq p_{zi} \leq r_z^+, \quad \forall z \in Z, i \in [N] \\ l_{zi}^+ &\leq \max\{0, -\delta_{zi}\} \cdot u_i^+, \quad \forall z \in Z, i \in [N] \\ l_{zi}^- &\leq \max\{0, \delta_{zi}\} \cdot u_i^-, \quad \forall z \in Z, i \in [N] \\ -T_{ei}^- &\leq f_{ei} \leq T_{ei}^+, \quad \forall e \in E, i \in [N] \\ \sum_{i \in [N]} u_i^{+/-} &\leq \lfloor \epsilon^{+/-} N \rfloor \\ r^{+/-} &\geq 0, l^{+/-} \geq 0, u^{+/-} \in \{0, 1\}^N \end{aligned} \quad (4)$$

Here, $u_i^{+/-}$ denotes the binary variable representing³ whether or not $r^{+/-}$ is in $F_i^{+/-}$. When $u_i^+ = 1$, it indicates a failure to serve negative imbalances for scenario i , since upward reserves cover negative imbalances. Likewise, $u_i^- = 1$ indicates that downward reserves fail to serve positive imbalances for scenario i . Slack variables $l_{zi}^{+/-}$ are non-zero only when $u_i^{+/-} = 1$, representing that imbalances cannot be covered in scenario i for that zone.

Unfortunately, it is well known that formulations using the “big-M method” are not practical for solving problems to optimality, due to large LP relaxation gaps. However, (4) can be used for a heuristic method in order to find a feasible solution. In [11], for example, the authors first solve the LP relaxation of (4) and fix $u_i^{+/-}$ as 1 for the indices in which the optimal solutions for the LP relaxation $u_i^{*+/-}$ are in the sets of $\lfloor \epsilon^{+/-} N \rfloor$ largest values when the solutions $u_i^{*+/-}$ are sorted in a descending order.

B. Minimal Projection Formulation

Another way to reformulate the constraints (3b) is to represent $r^{+/-} \in F^{+/-}$ explicitly in the space of $r^{+/-}$. Let us define several concepts on graphs in order to derive the projected formulation compactly.

³We denote $F_i^{+/-}$ as the sets $F^{+/-}$ where all the random variables (δ_z , $T_{ei}^{+/-}$) are replaced by their realizations for scenario i ; namely $(\delta_{zi}, T_{ei}^{+/-})$.

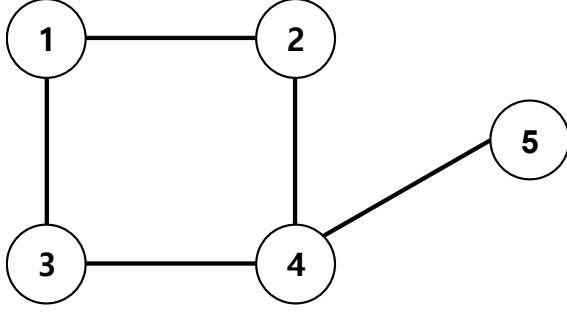


Fig. 1. A graph with 5 zones for illustrating the definition of a Connected Vertex Set.

Definition 2.1 (Connected Vertex Set): For a graph $\mathcal{G}(V, E)$, the connected vertex set $\mathcal{W}(\mathcal{G})$ is defined as follows:

$$\mathcal{W}(\mathcal{G}) = \{S \subseteq V : \forall v, w \in S, \\ \exists \text{ a path } P \text{ on } \mathcal{G} \text{ s.t. } v, w \in V(P) \subseteq S\}, \quad (5)$$

where $V(P)$ denotes the set of vertices in the path P .

Example 1 (Connected Vertex Set): For the graph in Fig. 1, $\{1, 2, 3\}$ is an element of a connected vertex set, whereas $\{1, 4\}$ is not. For a vertex set $\{1, 2, 3\}$, as an example, when $v = 2, w = 3$ there exists a path $3 \rightarrow 1 \rightarrow 2$ such that $v, w \in V(3 \rightarrow 1 \rightarrow 2) = \{1, 2, 3\} \subseteq \{1, 2, 3\}$. This is true for all possible combinations of $v, w \in \{1, 2, 3\}$, so this is an element of the connected vertex set. On the other hand, for a vertex set $\{1, 4\}$, when $v = 1, w = 4$ there is no such path whose vertex sets are subsets of $\{1, 4\}$, since all the paths between $v = 1$ and $w = 4$ contain either 2 or 3, which are not elements of $\{1, 4\}$.

Intuitively, if all the elements in a vertex set have an edge that connects these vertices to any of the other elements in the vertex set, such vertices are elements of a connected vertex set; hence the name of the definition. For the 5-zone example in Fig. 1, the connected vertex set is

$$\begin{aligned} \mathcal{W}(\mathcal{G}) = & \{\{1\}, \{2\}, \{3\}, \{4\}, \{5\}, \\ & \{1, 2\}, \{1, 3\}, \{2, 4\}, \{3, 4\}, \{4, 5\}, \\ & \{1, 2, 3\}, \{1, 2, 4\}, \{1, 3, 4\}, \{2, 3, 4\}, \{2, 4, 5\}, \{3, 4, 5\}, \\ & \{1, 2, 3, 4\}, \{1, 2, 4, 5\}, \{1, 3, 4, 5\}, \{2, 3, 4, 5\}, \{1, 2, 3, 4, 5\}\}, \end{aligned}$$

and the size of the connected vertex set $|\mathcal{W}(\mathcal{G})|$ is 21.

Definition 2.2 (Maximum Input/Output Flow): For a directed graph $\mathcal{G}(V, E)$ where $\forall e \in E, f(e)$ denotes the flow in e and $-T_e^- \leq f(e) \leq T_e^+$, for all $S \subseteq V, E' \subseteq E$, the Maximum Input Flow $I(S|E')$ and the Maximum Output Flow $O(S|E')$ on E' are defined as follows:

$$I(S|E') = \sum_{v \in S, w \in S^c: (v, w) \in E'} T_{(v, w)}^- + \sum_{v \in S, w \in S^c: (w, v) \in E'} T_{(w, v)}^+, \quad (6)$$

$$O(S|E') = \sum_{v \in S, w \in S^c: (v, w) \in E'} T_{(v, w)}^+ + \sum_{v \in S, w \in S^c: (w, v) \in E'} T_{(w, v)}^-. \quad (7)$$

Example 2 (Maximum Input/Output Flow): In Fig. 2, every edge of the directed graph has flow capacities in both directions. For the edge $(1, 2)$, the maximum capacity for the direction $1 \rightarrow 2$ is $T_{(1, 2)}^+$, and the maximum capacity for the

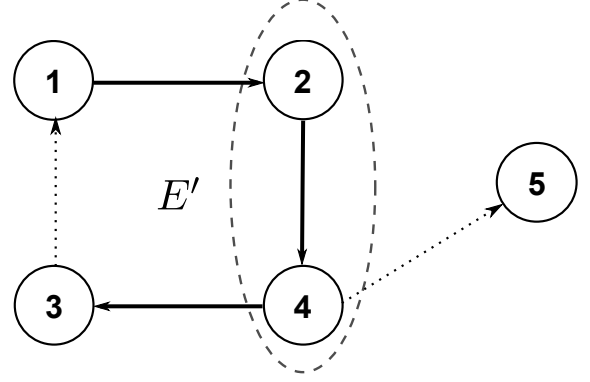


Fig. 2. A directed graph for illustrating Maximum Input/Output Flow.

direction $2 \rightarrow 1$ is $T_{(1, 2)}^-$. Maximum Input/Output Flows are defined on an edge subset $E' = \{(1, 2), (2, 4), (4, 3)\} \subset E$ for a vertex subset S . In Fig. 2, $S = \{2, 4\}$, so the Maximum Input Flow is $I(S|E') = T_{(1, 2)}^+ + T_{(4, 3)}^-$, and the Maximum Output Flow is $O(S|E') = T_{(1, 2)}^- + T_{(4, 3)}^+$.

Let us return to our problem. For the sake of brevity, let us denote $\mathcal{W}(\mathcal{G}(Z, E))$ for the network $\mathcal{G}(Z, E)$ for our original problem as $\mathcal{W}(\mathcal{G})$ from now on. Using this new notation, we define the three following sets F, F_p, F_r . Here, $F = F^+ \cap F^-$ from (1) and (2). Since the proof for the set F is more general than the proofs for F^+ or F^- , we present the proof for F in this section.

$$F = \{(r^+, r^-, p, f) \in \mathbb{R}_+^{|Z|} \times \mathbb{R}_+^{|Z|} \times \mathbb{R}^{|Z|} \times \mathbb{R}^{|E|} : (8) - (10)\}$$

$$p_z + \delta_z = \sum_{e=(z, \cdot) \in E} f_e - \sum_{e=(\cdot, z) \in E} f_e, \quad z \in Z \quad (8)$$

$$-r_z^- \leq p_z \leq r_z^+, \quad z \in Z \quad (9)$$

$$-T_e^- \leq f_e \leq T_e^+, \quad e \in E \quad (10)$$

$$F_p = \{(r^+, r^-, p) \in \mathbb{R}_+^{|Z|} \times \mathbb{R}_+^{|Z|} \times \mathbb{R}^{|Z|} : (11) - (12)\}$$

$$-I(S|E) \leq \sum_{z \in S} (p_z + \delta_z) \leq O(S|E), \quad S \in \mathcal{W}(\mathcal{G}) \quad (11)$$

$$-r_z^- \leq p_z \leq r_z^+, \quad z \in Z \quad (12)$$

$$F_r = \{(r^+, r^-) \in \mathbb{R}_+^{|Z|} \times \mathbb{R}_+^{|Z|} : (13) - (14)\}$$

$$\sum_{z \in S} r_z^- \geq \sum_{z \in S} \delta_z - O(S|E), \quad S \in \mathcal{W}(\mathcal{G}) \quad (13)$$

$$\sum_{z \in S} r_z^+ \geq -\sum_{z \in S} \delta_z - I(S|E), \quad S \in \mathcal{W}(\mathcal{G}) \quad (14)$$

From now on, for a set A defined in the space of variables (x, y) , we denote $Proj_{(x)}(A)$ as the projection of the set A onto the space of x .

Theorem 2.1: $Proj_{(r^+, r^-)}(F) = F_r$.

Proof. The proof will be based on two steps. First, in Claim 2.1.2, we will show that the projection of F onto the space of (r^+, r^-, p) is F_p . Second, in Claim 2.1.1, we will show that the projection of F_p onto the space of (r^+, r^-) is F_r . Claim 2.1.2 and Claim 2.1.1 together imply that $Proj_{(r^+, r^-)}(F) = F_r$. Q.E.D.

Claim 2.1.1: $Proj_{(r^+, r^-)}(F_p) = F_r$.

Claim 2.1.2: $Proj_{(r^+, r^-, p)}(F) = F_p$.

The proof for Claim 2.1.1 is provided in the appendix. The proof for Claim 2.1.2 follows a similar reasoning but is more complex. For the sake of brevity, it is provided in [32].

Corollary 2.2: $Proj_{(r^{+/-})}(F^{+/-}) = F_r^{+/-}$, where

$$F_r^- = \{r^- \in \mathbb{R}_+^{|Z|} : (13)\}, F_r^+ = \{r^+ \in \mathbb{R}_+^{|Z|} : (14)\}.$$

Theorem 2.1 and Corollary 2.2 show that the set F_r (or $F_r^{+/-}$) is indeed an explicit representation of the projection of F (or $F^{+/-}$) on the space of the first stage variables $r^{+/-}$.

Theorem 2.3: F_r is a minimal representation on the space of (r^+, r^-) .

Corollary 2.4: $F_r^{+/-}$ is a minimal representation on the space of $r^{+/-}$.

Theorem 2.3 and Corollary 2.4 show that the sets of inequalities (13) and (14) are indeed minimal representations for the projection of F (or $F^{+/-}$). The proof for Theorem 2.3 is provided in [32].

Thanks to Corollary 2.2, the representation $r^{+/-} \in F^{+/-}$ in constraint (3b) can be replaced by (13) and (14) respectively. The resulting new formulation is only made up of the first-stage variables. Now that we have derived an explicit representation with inequalities, this new formulation enables us to apply Integer Programming techniques for joint chance-constrained programs. The fact that the representations are minimal is important, because the performance for joint chance-constrained programs depends significantly on the number of constraints that are contained in the probabilistic constraints. Thanks to Corollary 2.4, we are guaranteed that our representation is minimal, so that the number of constraints within the probabilistic constraints is minimized. In the following section, we introduce an extended formulation for this minimal projection formulation using one such IP technique.

III. STRENGTHENED FORMULATION

As we have discussed in section II.A, the “big-M method” is not practical as a formulation aiming for solving our problem to optimality, due to its large LP relaxation gap. Instead, in this section, we introduce Integer Programming techniques which enable us to solve the problem to optimality by making the LP relaxation gap much smaller. This approach also uses the sample approximation scheme in [13]. Let us reformulate (3) into (15) using the sample approximation for the rest of the paper.

$$\min \sum_{z \in Z} (r_z^+ + r_z^-) \quad (15a)$$

$$\text{s.t. } u_i^{+/-} = 0 \implies r^{+/-} \in F_i^{+/-}, \quad \forall i \in [N] \quad (15b)$$

$$\sum_{i \in N} u_i^{+/-} \leq \lfloor \epsilon N \rfloor \quad (15c)$$

$$r^{+/-} \geq 0, u^{+/-} \in \{0, 1\}^N \quad (15d)$$

First, we start from introducing mixing sets and mixing inequalities, which are building blocks of the IP techniques related to chance-constrained problems. Second, we show a technique directly applicable to two-stage chance-constrained problems. Third, we present another technique that can be applied to joint chance-constrained problems. Finally, using this technique, we strengthen our minimal projection formulation in section II.B.

A. Mixing Inequalities

With the reformulation (15) using sample approximation, we typically face mixing sets and mixing inequalities. Given N scalars h_i for $i \in [N]$, a mixing set is defined as

$$P = \{(y, u) \in \mathbb{R}_+ \times \{0, 1\}^N : y + h_i u_i \geq h_i, i \in [N]\}. \quad (16)$$

For a probabilistic constraint $\Pr\{y \geq h\}$, where h is a random variable and h_i denotes a sample of the random variable for all $i \in [N]$, when we apply the sample approximation approach the resulting set corresponds to the mixing set (16) depending on how we reformulate (15b) plus a knapsack or a cardinality constraint such as (15c). Here, the binary variable u_i denotes that the constraint $y \geq h$ is violated for the sample i when $u_i = 1$. This can be extended to more complex problems, such as two-stage or joint chance-constrained problems. Thus, techniques developed for a mixing set can be applied to these more complex problems.

Mixing inequalities, also named as star inequalities, are developed by Atamturk et. al [30] and Gunluk and Pochet [31]. If we assume that $h_1 \geq h_2 \geq \dots \geq h_N$ without loss of generality, the mixing inequalities for the mixing set (16) are defined as

$$y + \sum_{j=1}^l (h_{t_j} - h_{t_{j+1}}) u_{t_j} \geq h_{t_1}, \forall \{t_1, \dots, t_l\} \subset [N], \quad (17)$$

where $t_1 < \dots < t_l$ and $h_{t_{l+1}} := 0$. It is known that the mixing inequalities are valid and are sufficient for defining the convex hull of the mixing set (16). Defining a convex hull with a certain set of inequalities implies that the LP relaxation gap is zero, in other words, we can solve the Integer Programming problem by solving a Linear Programming problem with these convex hull defining inequalities. This fact can be used even for more complex problems in which we are not necessarily able to characterize the convex hull of the problem. When problems are more complex, we can no longer guarantee a zero LP relaxation gap; however, these mixing inequalities are still valid for those problems and this aids significantly in reducing the LP relaxation gap, resulting in better performance for solving the original Integer Programming problem with binary variables u .

Furthermore, for the following set with a cardinality constraint⁴ induced by a reliability criterion ϵ , where we define $q = \lfloor \epsilon N \rfloor$,

$$G = \{(y, u) \in \mathbb{R}_+ \times \{0, 1\}^N : \sum_{i=1}^N u_i \leq q, \\ y + h_i u_i \geq h_i, i \in [N]\}, \quad (18)$$

the strengthened mixing inequalities

$$y + \sum_{j=1}^l (h_{t_j} - h_{t_{j+1}}) u_{t_j} \geq h_{t_1}, \forall \{t_1, \dots, t_l\} \subset [q] \quad (19)$$

with $t_1 < \dots < t_l$ and $h_{t_{l+1}} := h_{t_{q+1}}$ are facet-defining for $\text{conv}(G)$ if and only if $t_l = 1$ [14]. An inequality is

⁴In this paper, we assume that all the scenarios have equal probabilities. There are similar techniques for knapsack constraints for unequal probabilities. The readers who are interested are referred to [14].

facet-defining for $\text{conv}(G)$ when the inequality is crucial for defining the convex hull of the set G . It implies that these inequalities are expected to be the most effective for reducing the LP relaxation gap among similar types of inequalities, since the convex hull is the smallest convex set containing all the feasible solutions. In the next subsections, we show how to use these strengthened mixing inequalities for different types of chance-constrained problems.

B. A Branch-and-Cut Algorithm for a Two-Stage Chance-Constrained Problem

One way to address a two-stage chance-constrained problem directly is to use Benders' Decomposition [25] in order to transform (15b) into a form of mixing sets. The Benders Cuts are used in order to decompose a large problem into smaller problems by dividing variables into different groups. By connecting the second-stage and first-stage variables, these cuts enable us to reformulate the original two-stage problem into a form of linear inequalities. The cuts are added on-the-fly, while a Branch-and-Bound algorithm is running for dealing with binary variables. This overall process is called a Branch-and-Cut algorithm. General theories for the detailed process of how Branch-and-Cut algorithm is linked with Benders' Decomposition are introduced in [20]. According to different types of Benders Cuts, this process differs slightly. Benders Optimality Cuts are used when there are second-stage variables in the objective function (see [18]). Benders Feasibility Cuts are used for representing the feasible region of the first-stage variables depending on second-stage variables (see [17]).

For our problem, the second-stage variables do not appear in the objective function, so we only require Benders Feasibility Cuts. As an example, Benders Feasibility Cuts for F_i^+ can be obtained by solving (20), which is the dual problem of the feasibility checking problem for F_i^+ when \hat{r}^+ is given:

$$\begin{aligned} v_i(\hat{r}^+) = \max & - \sum_{z \in Z} (\hat{r}_z^+ \pi_z + \delta_{iz} \lambda_z) - \sum_{e \in E} (T_e^+ \mu_e^+ + T_e^- \mu_e^-) \\ \text{s.t. } & \pi_z - \lambda_z = 0, \quad \forall z \in Z \\ & \lambda_{z_t} - \lambda_{z_s} - \mu_e^+ + \mu_e^- = 0, \quad \forall e = (z_s, z_t) \in E \\ & \pi, \lambda \in [0, 1]^{|Z|}, \mu^+, \mu^- \in [0, 1]^{|E|} \end{aligned} \quad (20)$$

If $v_i(\hat{r}^+) > 0$, then $\hat{r}^+ \notin F_i^+$. Let $(\hat{\pi}, \hat{\lambda}, \hat{\mu}^+, \hat{\mu}^-)$ be an optimal extreme point solution of (20). Then, for

$$\begin{aligned} \alpha &= \hat{\pi}, \\ \beta &= -\delta_i \hat{\lambda} - T^+ \hat{\mu}^+ - T^- \hat{\mu}^-, \end{aligned} \quad (21)$$

$\alpha \hat{r}^+ < \beta$ and $\alpha r^+ \geq \beta$, for all $r^+ \in F_i^+$. We call this $\alpha r^+ \geq \beta$ a Benders Feasibility Cut.

The standard Benders Cuts are not directly applicable to our problem. The Benders Feasibility Cuts represent $r \in F_i$, but what we need is the cuts which represent the logical expression in (15b). In order to represent this implication, we formulate the following optimization problem for each scenario:

$$h_i^+(\alpha) := \min\{\alpha r^+ | r^+ \in F_i^+\}. \quad (22)$$

Here, $\alpha r^+ + h_i^+(\alpha) u_i^+ \geq h_i^+(\alpha)$ is a valid inequality for (15b), because if $u_i^+ = 0$, $r^+ \in F_i^+$, then $\alpha r^+ \geq h_i^+(\alpha)$ by definition

of $h_i^+(\alpha)$. A similar process can be applied to r^- and F_i^- : see [17] for the general theory, [12] for the application to our problem.

Indeed, the method explained above enables us to connect the logical expression (15b) to mixing sets (16), so that we can utilize the strengthened mixing inequalities (19). However, this direct approach is not applicable to large-scale realistic case studies. First, the cut generating process is computationally expensive, especially when there are many scenarios to consider, since every time we generate a cut we need to solve subproblems (22) for every scenario. Second, the resulting set of the inequalities representing the feasible set of the first-stage variables is not minimal. The number of mixing sets is crucial to the performance of solving Integer Programming, so this undermines the scalability of the resulting algorithm. For test results on a power systems application, the reader is referred to [12]. In the next subsection, we introduce a method that can be directly applied to a joint chance-constrained problem with only first-stage variables. Thanks to our minimal projection formulation that is derived in section II.B, we can resolve both of these issues.

C. A Strong Extended Formulation for a Joint Chance-Constrained Problem

Another way to deal with logical constraints (15b) is to represent $r^{+/-} \in F^{+/-}$ in terms of linear inequalities, in other words, to find a representation of the projection of $F^{+/-}$ in the space of $r^{+/-}$. This is already done in section II.B, and Corollary 2.4 shows that this representation is minimal. This is equivalent to the case where we apply the sample approximation to a joint chance-constrained problem (23), where T^+ and T^- are linear maps and there are uncertainties only in the right-hand-sides ξ^+ and ξ^- .

$$\begin{aligned} \min & \sum_{z \in Z} (r_z^+ + r_z^-) \\ \text{s.t. } & \Pr\{T^{+/-} r^{+/-} \geq \xi^{+/-}\} \geq 1 - \epsilon^{+/-} \\ & r^{+/-} \geq 0 \end{aligned} \quad (23)$$

Now, we can apply Integer Programming techniques for a joint chance-constrained problem with right-hand-side uncertainty, such as [14]–[16], [19], [21]–[24]. In this paper, we introduce a strong extended formulation from [14]. Although not the most recent method applicable, this method is easy to implement and achieves excellent performance for our application. This approach is further explored in [15]. Additional methods that are developed more recently can be added to this method if necessary.

Let us first define the extended formulation of G (18) with q additional binary variables w as follows:

$$\begin{aligned} EG &:= \{(y, u, w) \in \mathbb{R}_+ \times \{0, 1\}^{N+q} : \\ & \sum_{i=1}^N u_i \leq q, (25a) - (25c)\}, \end{aligned} \quad (24)$$

where

$$y + \sum_{i=1}^q (h_i - h_{i+1})w_i \geq h_1 \quad (25a)$$

$$w_i - w_{i+1} \geq 0, \quad \forall i \in [q-1] \quad (25b)$$

$$u_i - w_i \geq 0, \quad \forall i \in [q]. \quad (25c)$$

Theorem 3.1: (Theorem 6 from [14]) $\text{Proj}_{(r,u)}(EG) = G$. Moreover, the projection of the linear relaxation of EG is the linear relaxation of G .

Thus, by utilizing the extended formulation EG , we can have the same effect as adding the entire exponential family of valid inequalities (19). In the next section, we combine the minimal projection formulation in section II.B and the strong extended formulation technique introduced above.

IV. STRENGTHENED MINIMAL PROJECTION FORMULATION

A. Formulation

The strengthened minimal projection formulation using F_r ((13), (14)) and EG (24) is formally defined as follows:

$$\begin{aligned} \min \quad & \sum_{z \in Z} (r_z^+ + r_z^-) \\ \text{s.t.} \quad & \sum_{z \in S} r_z^{+/-} + \sum_{i=1}^{q^{+/-}} (h_{S,i}^{+/-} - h_{S,i+1}^{+/-})w_{S,i}^{+/-} \geq h_{S,1}^{+/-}, S \in \mathcal{W}(\mathcal{G}) \\ & w_{S,i}^{+/-} - w_{S,i+1}^{+/-} \geq 0, \quad \forall i \in [q^{+/-} - 1], S \in \mathcal{W}(\mathcal{G}) \\ & u_{\sigma_{S,i}^{+/-}}^{+/-} - w_{S,i}^{+/-} \geq 0, \quad \forall i \in [q^{+/-}], S \in \mathcal{W}(\mathcal{G}) \\ & \sum_{i=1}^N u_i^{+/-} \leq q^{+/-} \\ & r^{+/-} \geq 0, u^{+/-} \in \{0, 1\}^N, w^{+/-} \in \{0, 1\}^{q^{+/-} \cdot |\mathcal{W}(\mathcal{G})|}, \end{aligned} \quad (26)$$

where $q^{+/-} = \lfloor \epsilon^{+/-} N \rfloor$.

For $S \in \mathcal{W}(\mathcal{G})$,

$$h_{S,\sigma_{S,i}^+}^+ = - \sum_{v \in S} \delta_{v,i} - I_i(S|E) \quad (27a)$$

$$h_{S,\sigma_{S,i}^-}^- = \sum_{v \in S} \delta_{v,i} - O_i(S|E), \quad (27b)$$

where $\sigma_{S,i}^{+/-}$ are the permutations that rearrange the indices as $h_{S,1}^+ \geq h_{S,2}^+ \geq \dots \geq h_{S,N}^+$ and $h_{S,1}^- \geq h_{S,2}^- \geq \dots \geq h_{S,N}^-$, and for $i \in [N]$

$$\begin{aligned} I_i(S|E) = & \sum_{v \in S, w \in S^c: (v,w) \in E} T_{(v,w),i}^- \\ & + \sum_{v \in S, w \in S^c: (w,v) \in E} T_{(w,v),i}^+, \end{aligned} \quad (28)$$

$$\begin{aligned} O_i(S|E) = & \sum_{v \in S, w \in S^c: (v,w) \in E} T_{(v,w),i}^+ \\ & + \sum_{v \in S, w \in S^c: (w,v) \in E} T_{(w,v),i}^-. \end{aligned} \quad (29)$$

B. Implementation

The formulation (26) is a Mixed-Integer Linear Programming problem which can be directly solved by any commercial solver that offers a Branch-and-Bound algorithm such as CPLEX and GUROBI. There are many free solvers available

that provide Branch-and-Bound algorithm as well. However, in order to implement the algorithm, we require three elements: the connected vertex set $\mathcal{W}(\mathcal{G})$, the coefficients of mixing sets $h_{S,i}^{+/-}$ and the permutations $\sigma_{S,i}^{+/-}$ for all $S \in \mathcal{W}(\mathcal{G})$ and $i \in [N]$.

Algorithm 1 $\mathcal{W}(\mathcal{G})$ Generation

Input: $\mathcal{G} = (V, E)$

Output: \mathcal{W}

Select a start node $v_0 \in V$

Initialize $\mathcal{W} = \{\{v_0\}\}$, $V_{sel} = \{v_0\}$, $E_{sel} = \emptyset$

while $E_{sel} \neq E$ **do**

 Choose $e = (v, w) \in E(V_{sel}) = \{e' \in E : \exists v' \in V_{sel} \text{ s.t. } e' = (v', \cdot) \text{ or } e' = (\cdot, v')\}$

$E_{sel} \leftarrow E_{sel} \cup \{e\}$

if $v, w \in V_{sel}$ **then**

$\mathcal{W}^v \leftarrow \{S \in \mathcal{W} : v \in S\}$

$\mathcal{W}^w \leftarrow \{S \in \mathcal{W} : w \in S\}$

for $S_1 \in \mathcal{W}^v, S_2 \in \mathcal{W}^w$ **do**

$\mathcal{W} \leftarrow \mathcal{W} \cup \{S_1 \cup S_2\}$

end for

else

 (WLOG assume $v \in V_{sel}$ and $w \notin V_{sel}$)

$\mathcal{W} \leftarrow \mathcal{W} \cup \{\{w\}\}$

$V_{sel} \leftarrow V_{sel} \cup \{w\}$

$\mathcal{W}^v \leftarrow \{S \in \mathcal{W} : v \in S\}$

for $S \in \mathcal{W}^v$ **do**

$\mathcal{W} \leftarrow \mathcal{W} \cup \{S \cup \{w\}\}$

end for

end if

end while

1) Generation of Connected Vertex Set: The connected vertex set of a graph $\mathcal{G} = (V, E)$ can be generated using algorithm IV-B1. The size of the resulting connected vertex set $\mathcal{W}(\mathcal{G})$ varies according to the topology of the graph \mathcal{G} . When the graph is radial and all the nodes are connected (such as chains), the size of the connected vertex set is minimal and it is $|\mathcal{W}(\mathcal{G})| = 1/2 \cdot |V|(|V| + 1)$. The worst-case scenario is when the graph is a complete graph where all the nodes are connected to each other. In this case, the size of the connected vertex set is $|\mathcal{W}(\mathcal{G})| = 2^{|V|} - 1$. For the graph in Fig. 1, there are 5 zones, so the size ($|\mathcal{W}(\mathcal{G})| = 21$) is within the range of $4 \cdot 5/2 = 10 \leq 21 \leq 2^5 - 1 = 31$.

The $\mathcal{W}(\mathcal{G})$ Generation algorithm presented in this paper has a worst-case complexity⁵ of $\mathcal{O}(|E| \cdot 2^{|V|})$. This is incomparably lower than the complexities of projection methods for general purposes. The complexity of the original Fourier-Motzkin-Elimination algorithm [26], well-known for a general projection method, is known for its double exponential complexity, that is $\mathcal{O}((|E| + |V|)^{2^{|E|+|V|}})$ for our case. A recently developed general algorithm [27] enjoys a single exponential complexity, but with much higher exponents; namely $\mathcal{O}((|E| + |V|)^{2.5(|E|+2|V|)} \cdot (|E| + 2|V|)^3)$ for our problem.

⁵The algorithm scans every $e \in E$, and for each e in a worst-case scenario it can scan all the pairs of $v \in V$ that has the complexity of $\mathcal{O}(2^{|V|})$.

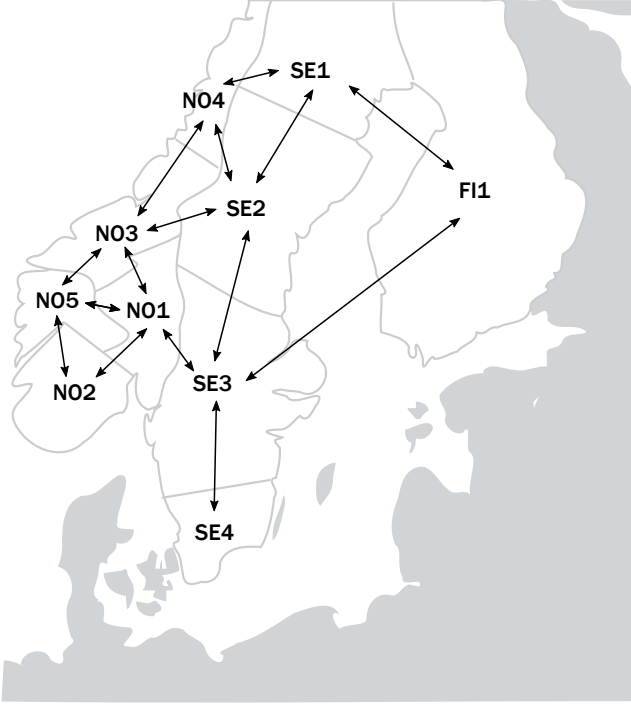


Fig. 3. Bidding zones and transmission network lines for a case study of the Nordic countries.

2) *Sorting*: Now that we have $|\mathcal{W}(\mathcal{G})|$, we are ready to generate the remaining elements $h_{S,i}^{+/-}$ and $\sigma_{S,i}^{+/-}$. An easy way to obtain such $h_{S,i}^{+/-}$, $\sigma_{S,i}^{+/-}$ is to calculate the right-hand-side for each scenario i in (27) and sort these right-hand side parameters in a non-increasing order. Then, the resulting non-increasing sequence becomes $h_{S,i}^{+/-}$ and the corresponding permutation of the indices becomes $\sigma_{S,i}^{+/-}$. As the size of the connected vertex set can be exponential with respect to the number of zones, the time for the process of calculating $h_{S,i}^{+/-}$ and $\sigma_{S,i}^{+/-}$ is non-negligible. In the next section, we present the calculation time for pre-processing as well as the solver time for the optimization problem when we present the computational results for a case study.

V. COMPUTATIONAL RESULTS

For the computational results, a case study of the Nordic system is considered. In this case study, as indicated in Fig. 3, three Nordic countries (Norway, Sweden and Finland) are involved and they account for 10 bidding zones with 15 links. The reference data for imbalances for each zone and the network capacity are sourced from [33]. For the imbalances, we generate samples from a normal distribution with zero mean and a standard deviation equal to the reference imbalances. For the network capacity, we add perturbations to the reference data for each sample. The perturbations are distributed according to a normal distribution with zero mean and a standard deviation equal to 5% of the value of the reference data. For all the figures 4 - 6, the bar charts refer to the mean of 100 simulations in which the middle lines indicate the standard deviation.

First, we compare the Strengthened Minimal Projection Method in section IV and the LP Based Heuristic Method in [11]. In Fig. 4, the results comparing (a) the optimal reserve sizes and (b) the total solving time are presented for varying degrees of reliability levels (ϵ) when the sample size is $N = 25,000$. The Minimal Projection Method can be solved incomparably faster than the LP Based Heuristic, *and* finds the optimal solution. This seemingly counter-intuitive result can be explained by the fact that the strengthened minimal projection formulation (26) often has a smaller size than the formulation (4) in terms of the number of variables and constraints. Notice that $q \ll N$, thus each set of constraints in (26) is repeated q times whereas that in (4) is N times. Additionally, even though the size of the connected vertex set $\mathcal{W}(\mathcal{G})$ is exponential, it is often the case that $h^{+/-}$ in (27) are all negative, resulting in adding redundant constraints that can be ignored or automatically removed in pre-processing steps of commercial optimization solvers. This phenomenon happens more often when the capacities of lines $T^{+/-}$ are sufficiently large compared to the level of imbalances $\delta^{+/-}$. Consider an extreme case where $T^{+/-}$ is infinity, then the only non-redundant constraints are when $S \in \mathcal{W}(\mathcal{G})$ is equal to the set of all the zones Z , which is equivalent to the case where we aggregate all the zones in one region.

The gap between the optimal solution and the sub-optimal solution from the LP method when $\epsilon = 1\%$ is around 18.9%. As ϵ becomes smaller, since q also becomes smaller, the optimization problem becomes less complex, resulting in a smaller gap between the optimal solution and the sub-optimal solution and a faster solving time. However, the high value of the standard deviation in the optimal solution for $\epsilon = 0.1\%$ implies that the sample size is not sufficient. When we increase the sample size, then the gap also increases.

Second, in Fig. 5, we present a sensitivity analysis result for the sample approximation approach over sample size for our case study. As in [13], insufficient numbers of samples result in an underestimation of the objective function value. This phenomenon can be observed in Fig. 5. Only when the sample size is larger than $N = 250,000$ does the optimal reserve size converge. When $N = 10,000$, we see not only the underestimation issue, but also a high level of coefficient of variation (1.1 %). As we increase the sample size, the standard deviation decreases and the value of reserve size stabilizes.

Lastly, we analyze the solving time for the Strengthened Minimal Projection Method over different sample sizes in Fig. 6. Notice that $\epsilon = 1\%$ is the most computationally complex problem among the three different levels of ϵ . Our method allows us to solve $N = 500,000$ samples in less than 30 minutes in terms of optimization time. In general, the data pre-processing time is non-negligible due to the exponential size of the connected vertex set $\mathcal{W}(\mathcal{G})$; however, the bottleneck complexity is $\mathcal{O}(N \log N)$ due to the sorting algorithm that is still scalable. In practice, if one needs to solve the problem dynamically, adding new samples to an already-sorted list (which is the case in practice) is much easier than sorting the entire lists, and in this case the data pre-processing time is negligible.

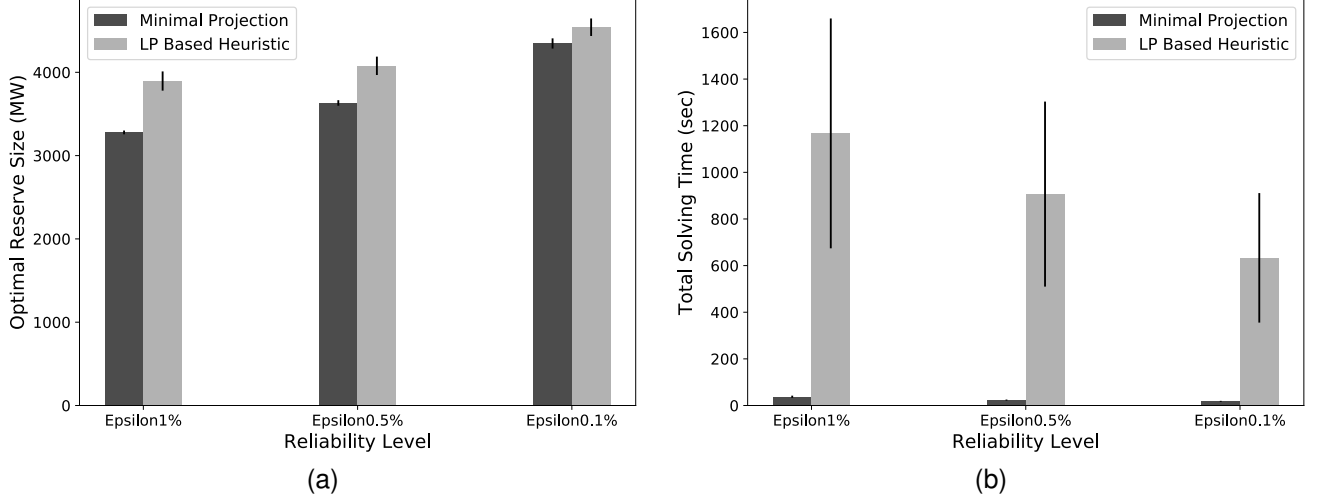


Fig. 4. Comparison between Strengthened Minimal Projection Method and the LP Based Heuristic Method when the sample size is $N = 25,000$ in terms of (a) optimal objective function value and (b) total solving time.

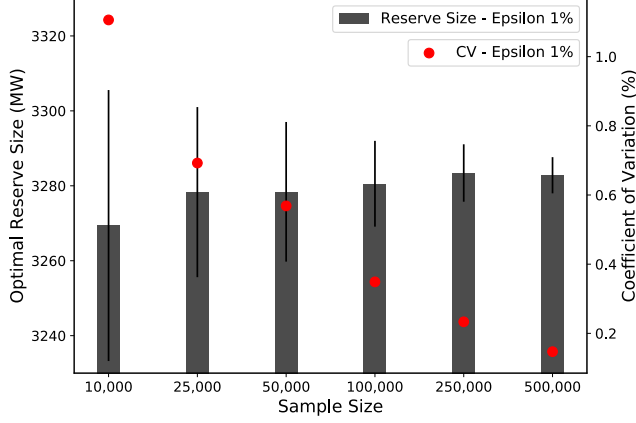


Fig. 5. Sensitivity analysis for the sample approximation approach over sample size when epsilon is 1%.

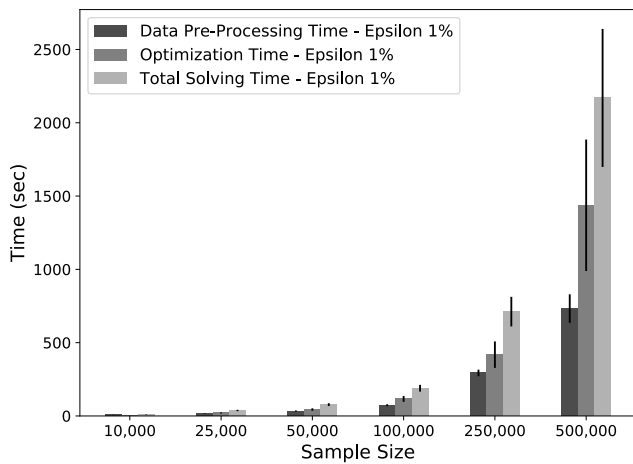


Fig. 6. Solving time for the Strengthened Minimal Projection Method over sample size when epsilon is 1%.

VI. CONCLUSION

In this article, we propose a novel method for solving the chance-constrained multi-area reserve sizing problem to optimality. Identifying a minimal representation of the projected set of our feasible region, we use integer programming methods to strengthen our formulation. This approach can deal with instances of realistic size, and this is shown in a case study of the Nordic system. Since a transportation-based network is used for our method, this approach can also be used in different domains.

In future work, it is possible to extend the model with different approximations of power balance equations. A DC (Direct Current) approximation can be an option. From the perspective of better calculation, we can apply more recent IP techniques for solving the minimal projection formulation.

ACKNOWLEDGMENTS

This work is inspired by a collaborative project between N-SIDE and the Swedish TSO Svenska kraftnät. The authors gratefully acknowledge the helpful supports from Olivier Devolder, Thomas Gueuning, and Alberte Bousso from N-SIDE.

APPENDIX PROOF OF CLAIM 2.1.1

In this appendix, we use V instead of Z as the vertex set in the set F_p and F_r .

Lemma A.1: For a graph $\mathcal{G}(V, E)$,

$$I(S_1 \setminus S_2 | E') + O(S_2 \setminus S_1 | E') \leq I(S_1 | E') + O(S_2 | E'), \\ \forall S_1, S_2 \subseteq V, E' \subseteq E.$$

Proof. For the compactness of the proof, without loss of generality, we leave out the conditions $(v, w) \in E'$ or $(w, v) \in$

E' under the summation sign. We can divide $I(S_1 \setminus S_2|E')$ into two terms:

$$I(S_1 \setminus S_2|E') = \sum_{v \in S_1 \setminus S_2, w \in S_1^c} (T_{(v,w)}^- + T_{(w,v)}^+) + \sum_{v \in S_1 \setminus S_2, w \in S_1 \cap S_2} (T_{(v,w)}^- + T_{(w,v)}^+). \quad (30)$$

Observe that since $S_1 \setminus S_2 \subseteq S_2^c$, the second term

$$\sum_{v \in S_1 \setminus S_2, w \in S_1 \cap S_2} (T_{(v,w)}^- + T_{(w,v)}^+) \leq \sum_{v \in S_2^c, w \in S_1 \cap S_2} (T_{(v,w)}^- + T_{(w,v)}^+). \quad (31)$$

By changing v and w , we can obtain

$$\sum_{v \in S_2^c, w \in S_1 \cap S_2} (T_{(v,w)}^- + T_{(w,v)}^+) = \sum_{v \in S_1 \cap S_2, w \in S_2^c} (T_{(v,w)}^+ + T_{(w,v)}^-). \quad (32)$$

In a similar way, $O(S_2 \setminus S_1|E')$ can be divided into two terms:

$$O(S_2 \setminus S_1|E') = \sum_{v \in S_2 \setminus S_1, w \in S_2^c} (T_{(v,w)}^+ + T_{(w,v)}^-) + \sum_{v \in S_2 \setminus S_1, w \in S_1 \cap S_2} (T_{(v,w)}^+ + T_{(w,v)}^-). \quad (33)$$

Since $S_2 \setminus S_1 \subseteq S_1^c$, the second term

$$\sum_{v \in S_2 \setminus S_1, w \in S_1 \cap S_2} (T_{(v,w)}^+ + T_{(w,v)}^-) \leq \sum_{v \in S_1^c, w \in S_1 \cap S_2} (T_{(v,w)}^+ + T_{(w,v)}^-). \quad (34)$$

By changing v and w , we can obtain

$$\sum_{v \in S_1^c, w \in S_1 \cap S_2} (T_{(v,w)}^+ + T_{(w,v)}^-) = \sum_{v \in S_1 \cap S_2, w \in S_1^c} (T_{(v,w)}^- + T_{(w,v)}^+). \quad (35)$$

Now observe that the sum of the first term of (30) and the right-hand-side of (35) is equal to $I(S_1|E')$. Likewise, the sum of the first term of (33) and the right-hand-side of (32) is equal to $O(S_2|E')$. Thus, $I(S_1 \setminus S_2|E') + O(S_2 \setminus S_1|E') \leq I(S_1|E') + O(S_2|E')$. Q.E.D.

Claim 2.1.1 $Proj_{(r^+, r^-)}(F_p) = F_r$.

Proof. First, we show that $Proj_{(r^+, r^-)}(F_p) \subseteq F_r$. From (12),

$$-\sum_{v \in S} r_v^- \leq \sum_{v \in S} p_v \leq \sum_{v \in S} r_v^+. \quad (39)$$

Now it is easy to see that (39) and (11) implies (13) and (14).

Second, we show that $F_r \subseteq Proj_{(r^+, r^-)}(F_p)$. It suffices to show that for all $(\hat{r}^+, \hat{r}^-) \in F_r$, there exists \hat{p} such that $(\hat{r}^+, \hat{r}^-, \hat{p}) \in F_p$. We show that we can find such \hat{p} from Algorithm A and it always exists. If it exists, it is easy to show that \hat{p} satisfies (12) from (36). Also, observe that \hat{p} satisfies (11) because for all $S \in \mathcal{W}(\mathcal{G})$, over the course of the while statement, there exists v, R such that $S \not\subseteq R, S \subseteq R \cup v$. Then (37) and (38) for S with such v, R become (11).

Now, we show the existence of such \hat{p} in Algorithm A. We use mathematical induction. Denote R_i and v_i as the node

Algorithm 2 Finding feasible \hat{p} to F_p from $(\hat{r}^+, \hat{r}^-) \in F_r$

Input: $\mathcal{G} = (V, E)$, $(\hat{r}^+, \hat{r}^-) \in F_r$

Output: \hat{p}

Start with an empty set $R \leftarrow \emptyset$

while $R \neq V$ **do**

 Choose $v \in V \setminus R$ such that $R \cup v \subseteq \mathcal{W}(\mathcal{G})$

 Fix \hat{p}_v satisfying (36) - (38)

$$-\hat{r}_v^- \leq \hat{p}_v \leq \hat{r}_v^+ \quad (36)$$

$$\hat{p}_v \geq -\sum_{w \in R \cap S} \hat{p}_w - \sum_{w \in S \setminus \{R \cup v\}} \hat{r}_w^+ - \sum_{w \in S} \delta_w - I(S|E), \quad S \in \mathcal{W}(\mathcal{G}) : v \in S \quad (37)$$

$$\hat{p}_v \leq -\sum_{w \in R \cap S} \hat{p}_w + \sum_{w \in S \setminus \{R \cup v\}} \hat{r}_w^- - \sum_{w \in S} \delta_w + O(S|E), \quad S \in \mathcal{W}(\mathcal{G}) : v \in S \quad (38)$$

$R \leftarrow R \cup v$

end while

sets and the nodes we get from Algorithm A as it iterates over the while statement. For the first step of the induction we consider the case where $R_1 = \emptyset$. The lower bound of (37) \leq the upper bound of (36) is implied by (14) and the upper bound of (38) \geq the lower bound of (36) is implied by (13). For showing why the lower bound of (37) \leq the upper bound of (38), pick $S_1, S_2 \in \{S \in \mathcal{W}(\mathcal{G}) : v_1 \in S\}$. From (13) for $S_2 \setminus S_1$ and (14) for $S_1 \setminus S_2$ ⁶ using Lemma A.1,

$$\begin{aligned} & \sum_{w \in S_1 \setminus S_2} r_w^+ + \sum_{w \in S_2 \setminus S_1} r_w^- \geq \\ & -\sum_{w \in S_1 \setminus S_2} \delta_w + \sum_{w \in S_2 \setminus S_1} \delta_w - I(S_1 \setminus S_2|E) - O(S_2 \setminus S_1|E) \\ & \geq -\sum_{w \in S_1 \setminus S_2} \delta_w + \sum_{w \in S_2 \setminus S_1} \delta_w - I(S_1|E) - O(S_2|E). \end{aligned} \quad (40)$$

Since $\sum_{w \in (S_1 \cap S_2) \setminus v_1} (r_w^+ + r_w^-) \geq 0$, (40) implies

$$\begin{aligned} & \sum_{w \in S_1 \setminus v_1} r_w^+ + \sum_{w \in S_2 \setminus v_1} r_w^- \geq \\ & -\sum_{w \in S_1} \delta_w + \sum_{w \in S_2} \delta_w - I(S_1|E) - O(S_2|E), \end{aligned} \quad (41)$$

which is equivalent to the lower bound of (37) for $S_1 \leq$ the upper bound of (38) for S_2 . Thus, \hat{p}_{v_1} satisfying (36) - (38) exists for the case where $R_1 = \emptyset$.

For the next step of mathematical induction, assume that for $i \geq 1$, there exists \hat{p}_{v_k} for $1 \leq k \leq i$ satisfying (36) - (38). For $R_{i+1} = R_i \cup v_i$ and $v_{i+1} \in V \setminus R_{i+1}$, our goal is to show that all the possible combinations of the upper bounds and the lower bounds from (36) - (38) can be implied by other inequalities so that we can show that $\hat{p}_{v_{i+1}}$ exists. First, we show it for the combinations of upper bounds and lower

⁶It is possible that $S_1 \setminus S_2 \notin \mathcal{W}(\mathcal{G})$ or $S_2 \setminus S_1 \notin \mathcal{W}(\mathcal{G})$, but in this case there exists disjoint $S_A, S_B \in \mathcal{W}(\mathcal{G})$ such that $S_A \cup S_B = S_1 \setminus S_2$ or $S_A \cup S_B = S_2 \setminus S_1$, and we can get the same results as (40) by summing up (13) or (14) for S_A and that for S_B .

bounds between (36) and (37) - (38). Here, we show one out of the two cases: the lower bound of (37) \leq the upper bound of (36). The other case can be shown in a similar fashion. The set $\mathcal{W}(\mathcal{G})$ can be divided into two cases : i) $R_{i+1} \cap S = \emptyset$ and ii) $R_{i+1} \cap S \neq \emptyset$. For the case i), $\sum_{w \in R_{i+1} \cap S} \hat{p}_w = 0$ and $\sum_{w \in S \setminus \{R_{i+1} \cup v_{i+1}\}} \hat{r}_w^+ = \sum_{w \in S \setminus v_{i+1}} \hat{r}_w^+$, so (14) implies the lower bound of (37) \leq the upper bound of (36). For the case ii), from the set $\{v : v \in R_{i+1} \cap S\}$, pick the node with the largest index l . Observe that $\sum_{w \in R_{i+1} \cap S} \hat{p}_w = \sum_{w \in R_l \cap S} \hat{p}_w + \hat{p}_{v_l}$ and $\sum_{w \in S \setminus R_{i+1}} \hat{r}_w^+ = \sum_{w \in S \setminus \{R_l \cup v_l\}} \hat{r}_w^+$. This can be proven by contradiction. Assume that it is not true. Then $\exists v_m$ such that $m \neq l, v_m \in R_{i+1}, v_m \notin R_l$, and $v_m \in S$. This contradicts the fact that l is the largest index. Thus, (37) with R_l and v_l implies the lower bound of (37) \leq the upper bound of (36).

For showing why the lower bound of (37) \leq the upper bound of (38), pick $S_1, S_2 \in \{S \in \mathcal{W}(\mathcal{G}) : v \in S\}$. We have four different cases to show : i) $R_{i+1} \cap S_1 = \emptyset, R_{i+1} \cap S_2 = \emptyset$, ii) $R_{i+1} \cap S_1 \neq \emptyset, R_{i+1} \cap S_2 = \emptyset$, iii) $R_{i+1} \cap S_1 = \emptyset, R_{i+1} \cap S_2 \neq \emptyset$, iv) $R_{i+1} \cap S_1 \neq \emptyset, R_{i+1} \cap S_2 \neq \emptyset$. Since it is similar in the other cases, here we only show the argument for the case ii) where $R_{i+1} \cap S_1 \neq \emptyset, R_{i+1} \cap S_2 = \emptyset$. From the set $\{v : v \in R_{i+1} \cap (S_1 \setminus S_2)\}$, pick the node with the largest index l . Similar to what we have shown above, observe that $\sum_{w \in R_{i+1} \cap (S_1 \setminus S_2)} \hat{p}_w = \sum_{w \in R_l \cap (S_1 \setminus S_2)} \hat{p}_w + \hat{p}_{v_l}$ and $\sum_{w \in (S_1 \setminus S_2) \setminus R_{i+1}} \hat{r}_w^+ = \sum_{w \in (S_1 \setminus S_2) \setminus \{R_l \cup v_l\}} \hat{r}_w^+$. From (37) for $S_1 \setminus S_2$ with R_l, v_l and (13) for $S_2 \setminus S_1$ using Lemma A.1, following a similar process as in (40) and (41) we get the inequality,

$$\sum_{w \in R_{i+1} \cap S_1} \hat{p}_w + \sum_{w \in S_1 \setminus R_{i+1}} r_w^+ + \sum_{w \in S_2} r_w^- \geq - \sum_{w \in S_1} \delta_w + \sum_{w \in S_2} \delta_w - I(S_1|E) - O(S_2|E), \quad (42)$$

which is equivalent to the lower bound of (37) for $S_1 \leq$ the upper bound of (38) for S_2 .

Thus, $\hat{p}_{v_{i+1}}$ satisfying (36) - (38) exists and it proves the existence of \hat{p} . Q.E.D.

REFERENCES

- [1] European Commission, "Commission regulation (EU) 2017/2195 of 23 november 2017 establishing a guideline on electricity balancing", *Tech. Rep.*, 2017.
- [2] T. Zheng, and E. Litvinov, "Contingency-based zonal reserve modeling and pricing in a co-optimized energy and reserve market", *IEEE transactions on Power Systems*, 23(2), 2008.
- [3] Y. Chen, P. Gribik, and J. Gardner, "Incorporating post zonal reserve deployment transmission constraints into energy and ancillary service co-optimization", *IEEE Transactions on Power Systems*, 29(2), 2013.
- [4] European Commission, "Commission regulation (EU) 2017/1485 of 2 august 2017 establishing a guideline on electricity transmission system operation", *Tech. Rep.*, 2017.
- [5] Nordic TSOs, "Nordic system operation agreement (SOA) - annex load-frequency control & reserves (LFCR)". [Online]. Available: https://eepublicdownloads.entsoe.eu/clean-documents/SOC%20documents/Nordic/Nordic%20SOA_Annex%20LFCR.pdf, 2019.
- [6] J.D. Lyon, K.W. Hedman, and M. Zhang, "Reserve requirements to efficiently manage intra-zonal congestion", *IEEE Transactions on Power Systems*, 29(1), 2013.
- [7] J. De Haan, M. Gibescu, D. Klaar, and W. Kling, "Sizing and allocation of frequency restoration reserves for LFC block cooperation", *Electric Power Systems Research*, 128, 2015.
- [8] C. Singh, P. Jirutitijaroen, and J. Mitra, "Electric power grid reliability evaluation: models and methods", *John Wiley & Sons*, 2018.
- [9] B. Park, Z. Zhou, A. Botterud, and P. Thimmapuram, "Probabilistic zonal reserve requirements for improved energy management and deliverability with wind power uncertainty", *IEEE Transactions on Power Systems*, 35(6), 2020.
- [10] F. Wang and Y. Chen, "Market implications of short-term reserve deliverability enhancement", *IEEE Transactions on Power Systems*, 36(2), 2021.
- [11] A. Papavasiliou, et al., "Multi-Area Reserve Dimensioning using Chance-Constrained Optimization", *IEEE Transactions on Power Systems*, 2021.
- [12] J. Cho, and A. Papavasiliou, "A branch-and-cut algorithm for chance-constrained multi-area reserve sizing", *UCLouvain CORE Discussion Paper*, 2022. <https://dial.uclouvain.be/pr/boreal/object/boreal:260463>
- [13] J. Luedtke, and S. Ahmed, "A sample approximation approach for optimization with probabilistic constraints", *SIAM Journal on Optimization*, 19(2), 2008.
- [14] J. Luedtke, S. Ahmed, and G.L. Nemhauser, "An integer programming approach for linear programs with probabilistic constraints", *Math. Program.*, 122(2), 2010.
- [15] J.P. Vielma, S. Ahmed, and G.L. Nemhauser, "Mixed integer linear programming formulations for probabilistic constraints", *Operations Research Letters*, 40(3), 2012.
- [16] S. Küçükyavuz, "On mixing sets arising in chance-constrained programming", *Math. Program.*, 132(1), 2012.
- [17] J. Luedtke, "A branch-and-cut decomposition algorithm for solving chance-constrained mathematical programs with finite support", *Math. Program.*, 146(1), 2014.
- [18] L. Xiao, S. Küçükyavuz, and J. Luedtke, "Decomposition algorithms for two-stage chance-constrained programs", *Math. Program.*, 157(1), 2016.
- [19] A. Ahmad, and R. Fukasawa, "On the mixing set with a knapsack constraint", *Math. Program.*, 157(1), 2016.
- [20] S. Küçükyavuz, and S. Suvrajeet, "An introduction to two-stage stochastic mixed-integer programming", *Leading Developments from INFORMS Communities*, 2017.
- [21] M. Zhao, H. Kai, and B. Zeng, "A polyhedral study on chance constrained program with random right-hand side", *Math. Program.*, 166(1), 2017.
- [22] W. Xie, and S. Ahmed, "On quantile cuts and their closure for chance constrained optimization problems", *Math. Program.*, 172(1), 2018.
- [23] L. Xiao, F. Kılınç-Karzan, and S. Küçükyavuz, "On intersection of two mixing sets with applications to joint chance-constrained programs", *Math. Program.*, 175(1), 2019.
- [24] F. Kılınç-Karzan, S. Küçükyavuz, and D. Lee, "Joint chance-constrained programs and the intersection of mixing sets through a submodularity lens", *Math. Program.*, 2021.
- [25] J.F. Benders, "Partitioning procedures for solving mixed-variables programming problems", *Numerische mathematik*, 4(1), 1962.
- [26] T.S. MOTZKIN, "Beitrage zur theorie der linearen Ungleichungen", Doctoral Thesis, University of Base, 1936.
- [27] R.J. Jing, M. Moreno-Maza, and D. Talaashrafi, "Complexity estimates for fourier-motzkin elimination", International Workshop on Computer Algebra in Scientific Computing, *Springer*, 2020.
- [28] ACER, "ACER decision on the implementation framework for mFRR platform: Annex I. implementation framework for the European platform for the exchange of balancing energy from frequency restoration reserves with manual activation in accordance with article 20 of commission regulation (EU) 2017/2195 of 23 November 2017 establishing a guideline on electricity balancing", *Tech. Rep.*, 2020.
- [29] A. Papavasiliou et al, "Hierarchical Balancing in Zonal Markets", *2020 17th International Conference on the European Energy Market (EEM)*, 2020.
- [30] A. Atamtürk, G.L. Nemhauser, and M.W. Savelsbergh, "The mixed vertex packing problem", *Math. Program.*, 89(1), 2000.
- [31] O. Günlük, and Y. Pochet, "Mixing mixed-integer inequalities", *Math. Program.*, 90(3), 2001.
- [32] J. Cho, "Proofs of theorems in exact mixed-integer programming approach for chance-constrained multi-area reserve sizing", *Tech. Rep.*, 2022. <https://jcho.eu/files/MultiAreaReserveSizingProofs.pdf>
- [33] J. Boe, "Balancing energy activation with network constraints", Master Thesis, *Norwegian University of Science and Technology*, 2017. https://ntnuopen.ntnu.no/ntnu-xmlui/bitstream/handle/11250/2453070/17422_FULLTEXT.pdf?sequence=1&isAllowed=y